NJC

ROYAL SOCIETY OF CHEMISTRY

PAPER

View Article Online
View Journal | View Issue

Cite this: *New J. Chem.*, 2020, **44**, 13007

CK2 inhibition, lipophilicity and anticancer activity of new N^1 *versus* N^2-substituted tetrabromobenzotriazole regioisomers†

Ahmed El-Kardocy,[a] Yaser A. Mostafa,[b] Noha G. Mohamed,[a] Mohammad Nabil Abo-Zeid,[c] Nivin A. Hassan,[d] Helal F. Hetta[ef] and Abu-Baker M. Abdel-Aal *[ab]

A new series of antiproliferative casein kinase 2α (CK2α) inhibitors were synthesized incorporating either a hydrophilic group (carboxylic or hydrazide) or a hydrophobic group (ester) at N^1 or N^2 of 4,5,6,7-tetrabromobenzotriazole (TBBt). New compounds were prepared *via* *N*-alkylation of TBBt followed by base-catalysed hydrolysis or hydrazinolysis. All the compounds demonstrated low sub-micromolar inhibition of CK2α and antiproliferative activity against both breast and lung cancer cell lines (MCF-7, and A549, respectively), at low micromolar concentrations with N^2-regioisomers exhibiting higher activity than their corresponding N^1-isomers. The most active compound incorporates an acetic acid hydrazide moiety at the N^2 of the TBBt triazole nucleus with IC_{50} at 0.131 μM (CK2α), 9.1 μM (MCF-7) and 6.3 μM (A549). It induced apoptosis in the MCF-7 cell line through upregulation of bax (pro-apoptotic gene) four to five times higher than the corresponding ester or acid analogues. Molecular docking suggests that the hydrophilic group at N^2 of the TBBt triazole nucleus provides binding with important residues (Asp175, Lys68 and Trp176) in the ATP binding site of the CK2α enzyme. We are the first to experimentally estimate the lipophilicity of TBBt derivatives. Our study demonstrated that TBBt hydrazides are more lipophilic than their corresponding acids in contrast to the contradicting calculated lipophilicity using four well-known software programs. This may explain the higher anticancer activity of the most active hydrazide over its corresponding acid despite their nearly equipotent enzyme inhibition.

Received 9th March 2020,
Accepted 2nd July 2020

DOI: 10.1039/d0nj01194k

rsc.li/njc

1. Introduction

Oncogenic transformations are associated with activation and overexpression of several protein kinases involved in the regulation of critical cellular processes such as growth, differentiation, signalling and transduction.[1,2] Protein kinases activate other proteins by transferring a phosphate group from adenosine triphosphate (ATP) to serine, threonine or tyrosine in these proteins.[3] Inhibition of protein kinases is becoming the most attractive therapeutic strategy with over 20 kinase-targeting drugs having been approved as anticancer agents over the past decade and hundreds are currently in clinical trials for various diseases.[4–6] For instance, casein kinase 2 (CK2) is a serine/threonine protein kinase overexpressed in many cancers including acute myeloid leukaemia, and breast, prostate and lung cancers.[7,8] In the last decade, a great number of CK2 inhibitors have been developed including polyhalogenated benzimidazoles, polyhalogenated benzotriazoles, indolo and pyrroloquinolines with the most successful example, silmitasertib (CX-4945, Fig. 1), currently in clinical trials (ClinicalTrials.gov identifier: NCT02128282).[9–17]

[a] *Student Research Unit, Faculty of Pharmacy, Assiut University, Assiut 71526, Egypt. E-mail: abubaker.elsayed@pharm.aun.edu.eg; Tel: +02-0101-932-9596*
[b] *Department of Pharmaceutical Organic Chemistry, Faculty of Pharmacy, Assiut University, Assiut 71526, Egypt*
[c] *Department of Pharmaceutical Analytical Chemistry, Faculty of Pharmacy, Assiut University, Assiut 71526, Egypt*
[d] *Cancer Biology Department, South Egypt Cancer Institute, Assiut University, Assiut, Egypt*
[e] *Department of Medical Microbiology and Immunology, Faculty of Medicine, Assiut University, Assiut, Egypt*
[f] *Department of Internal Medicine, University of Cincinnati College of Medicine, Cincinnati, OH, USA*

† Electronic supplementary information (ESI) available: S1: Molecular modelling and docking with CK2α, S2: Cell viability of adenocarcinoma cell lines treated with 0–20 μM of compound **5** for 48 h; Table S3: The R_{M0} values, *C* (the percentage of ACN), *b* (slope) and *r* (correlation coefficient) of the equation $R_M = R_{M0} + bC$ for the studied compounds; Table S4: The R_{M0} values, *C* (the percentage of acetone), *b* (slope) and *r* (correlation coefficient) of the equation $R_M = R_{M0} + bC$ for the studied compounds; Table S5: The R_{M0} values, *C* (the percentage of MeOH), *b* (slope) and *r* (correlation coefficient) of the equation $R_M = R_{M0} + bC$ for the studied compounds. Fig. S6: IR, ^{1}H-NMR and ^{13}C-NMR spectra. See DOI: 10.1039/d0nj01194k

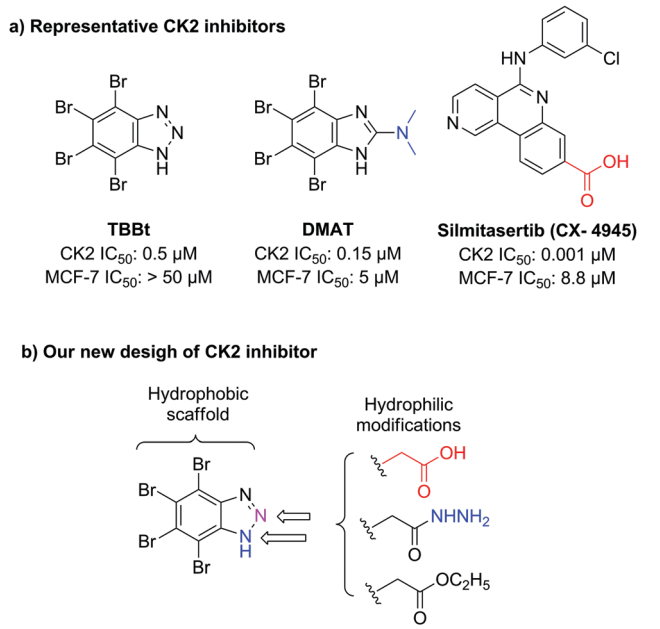

Fig. 1 Design of new anti-proliferative CK2 inhibitors. The polar ester, hydrazide or acid functional groups are introduced at either N^1 or N^2 of the TBBt scaffold.

4,5,6,7-Tetrabromo-1*H*-benzotriazole (TBBt, Fig. 1) is the most potent and selective CK2 inhibitor (K_i = 0.4 μM) among polyhalogenated benzotriazoles and second after DMAT among the polyhalogenated benzimidazoles.[18–21] The catalytic center of CK2α is relatively smaller than the active sites of other kinases.[22] The presence of four bromine atoms is optimal for binding of the molecule to a hydrophobic pocket in the ATP-binding site of the enzyme forming halogen bonds and hydrophobic interactions with essential hydrophobic amino acid residues.[23,24] Despite the potency and selectivity of TBBt as a CK2 inhibitor, it was found to be of low anti-proliferative potency and does not affect cell viability of cancer cell lines below 50 μM.[25] The human clinical trial candidate CX-4945 (Fig. 1), which is structurally unrelated to polyhalogenated benzotriazole, occupies the same hydrophobic pocket in the ATP binding site of CK2α.[13,25,26] The carboxyl group of CX-4945 is strategically positioned to provide extra hydrophilic interactions between CX-4945 and CK2α (Lys68, Glu81, Asp175 and Trp176), which is not possible in the case of TBBt.[13,26,27]

In the current study, we envisaged that the introduction of polar hydrophilic moieties (carboxyl acid or hydrazide) at the TBBt triazole ring (Fig. 1) may provide novel derivatives capable of forming strong polar interactions with the area outside the hydrophobic pocket of the CK2 ATP binding site compared to their hydrophobic ester analogues. Introduction of the polar groups at N^1 or N^2 of the triazole nucleus would give information about the importance of their orientation in the ATP binding site for CK2 inhibitory activity. Hydrophilic groups will alter important physicochemical properties of the polyhalogenated benzotriazole scaffold such as lipophilicity, which affect their cell membrane penetration and anti-proliferative activity. To the best of our knowledge, there are no reports on experimentally estimated lipophilicity of polyhalogenated benzotriazole derivatives.

In the current study, we report the lipophilicity of TBBt and our new N^1 and N^2-substituted TBBt regioisomers as estimated theoretically and experimentally to find correlations between lipophilicity and anticancer activity. The aim was to modify the polyhalogenated benzotriazole scaffold with a minimal polar functional group to improve CK2 inhibitory activity and to obtain polyhalogenated TBBt derivatives capable of inhibiting cancer cell proliferation at low concentrations.

2. Results and discussion

2.1. Chemistry

4,5,6,7-Tetrabromobenzotriazole (**1**) was synthesized *via* extensive bromination of benzotriazole in refluxing concentrated nitric acid as previously reported.[28] New target compounds **2–7** were efficiently synthesized *via* *N*-alkylation followed by hydrazinolysis or base catalyzed hydrolysis, Scheme 1. *N*-Alkylation was achieved by refluxing **1** with ethyl chloroacetate in acetone, potassium carbonate and tetrabutyl ammonium bromide as a phase transfer catalyst. A mixture of N^1 and N^2-acetate regioisomers (**2** and **3**) was obtained in a ratio of 3 : 2 in a good total yield. Separation of these two regioisomers was successfully performed by silica gel column chromatography and gradient elution of hexane : ethyl acetate (12 : 1 to 7 : 1). *N*-Alkylation was confirmed by the appearance of ester carbonyl group and aliphatic C–H stretching vibrations in the IR spectrum of **2** (1734.6 and 2925.2 cm^{-1}) and **3** (1743.2, 2967.9 cm^{-1}). Additionally, the *N*-methylene protons appear as singlet peaks at 5.89 and 5.94 ppm in the ^{1}H-NMR spectrum of **2** and **3**, respectively. While the two isomers exhibit quite similar IR and ^{1}H-NMR spectra, their ^{13}C-NMR spectra (Fig. 2) are fundamentally distinguishable. For instance, the N^1-acetate isomer (**2**) has six peaks in the aromatic region (100–150 ppm) corresponding to the benzotriazole ring carbons. In contrast, the N^2-acetate isomer (**3**) has only three peaks in the same region due to the existence of a plane of molecular symmetry.

Having the two esters in hand, we were able to obtain the corresponding hydrazides and acids. Hydrazinolysis was achieved by refluxing each ester (**2–3**) in excess hydrazine hydrate and ethanol for 6 h. Pure hydrazide derivatives (**4–5**) simply crystallized out when the reaction was left to cool overnight and obtained in a satisfactory yield by simple filtration and washing with ethanol. Hydrazides were identified by the appearance of NH and carbonyl vibrations in the IR spectra of **4** (3316 and 1663 cm^{-1}) and **5** (3304 and 1661 cm^{-1}). Moreover, the ethyl protons of the starting esters disappear in the ^{1}H-NMR spectra of the product hydrazides. Instead, additional peaks appear at 4.4 ppm and 9.5 ppm corresponding, respectively, to the NH_2 and NH protons with upfield shifting of the *N*-methylene protons to 5.51 ppm. The acid derivatives (**6–7**) were obtained by base-catalyzed hydrolysis of the corresponding esters (**2–3**) using 5% KOH. The products were obtained pure after acidification of the reaction mixture and were confirmed by the appearance of broad OH stretching vibration at 3200–2500 cm^{-1} and acid carbonyl stretching vibrations at

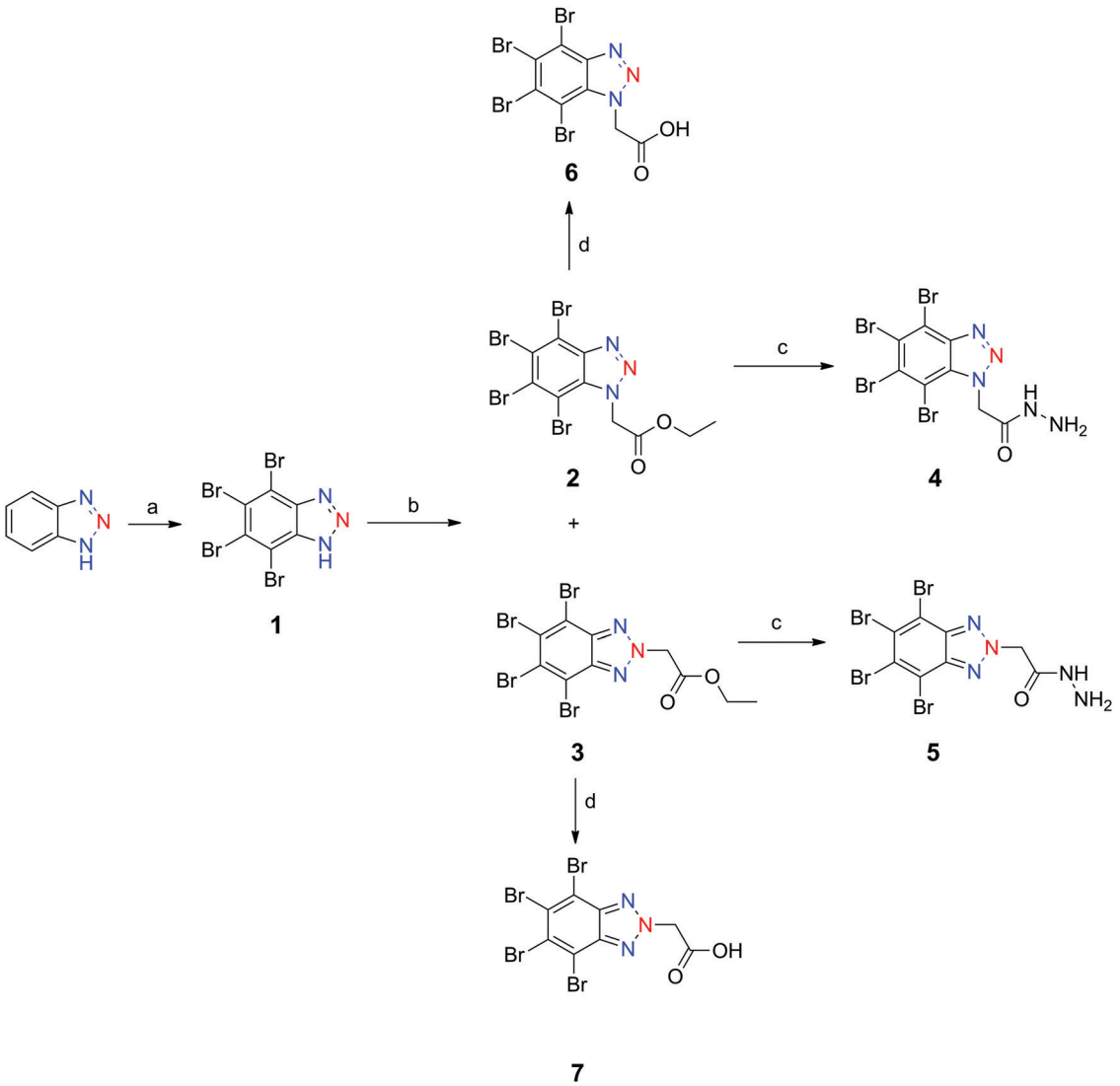

Scheme 1 Synthesis of N^1 and N^2-substituted TBBt regioisomers (**2–7**). *Reagents and conditions*: (a) Br_2, and conc. HNO_3, and reflux for 48 h; (b) $ClCH_2COOCH_2CH_3$, K_2CO_3, and acetone, and reflux for 6 h; (c) $NH_2NH_2{\cdot}H_2O$, and ethanol, and reflux for 6 h; (d) 5% KOH, and 50% aqueous ethanol, and reflux for 1 h.

1736 and 1732 cm^{-1} in the IR spectra of **6** and **7**, respectively. The ^{1}H-NMR spectra of both compounds show only one singlet peak for the *N*-methylene at 5.7–5.8 ppm. The purity of all the compounds was confirmed by elemental analysis and was found to exceed 99.6%.

2.2. CK2 enzyme inhibition and molecular modelling study

All tested compounds have the TBBt scaffold and differ only in the position and nature of the substituent at the triazole N^1 or N^2. Except for compound **2**, other tested compounds showed CK2 inhibitory activity at sub-micromolar concentrations (Fig. 3a).

The most potent derivatives (**5** and **7**) were five times more potent than the parent TBBt (**1**) with their CK2 IC50 at 0.131 and 0.098 μM, respectively. Both the compounds have their hydrophilic groups (hydrazide and carboxyl) substituted at N^2 of the triazole nucleus. Their respective regioisomers (**4** and **6**) were four to five times less potent, which indicates the importance of the position of the hydrophilic group for CK2 enzyme inhibitory activity. Similarly, ester derivatives (**2** and **3**) were three to four times less potent than their corresponding acid derivatives (**6** and **7**).

Molecular modelling study was done to explain the differences in the CK2 enzymatic inhibitory activities of the tested compounds in comparison to CX-4549. For instance, CX-4549 binds to key amino acids in the ATP binding site of CK2α including direct binding to Val116 and Lys68 and indirect binding *via* two conserved water molecules to Asp175, Glu81 and Trp176.[26] Docking of compounds **2–7** showed that these compounds occupy the same hydrophobic pocket in the CK2 ATP binding site like their parent compound (**1**) and CX-4945 (Fig. 3b and c, ESI† S2). The most potent CK2 enzyme inhibitors of the tested compounds (**5** and **7**) establish the essential direct interactions with Val116, Lys68 and Asp175 and indirect interactions with Glu81 and Trp176 through two water molecules. The triazole ring forms hydrophobic interaction with Val66 (**5**)

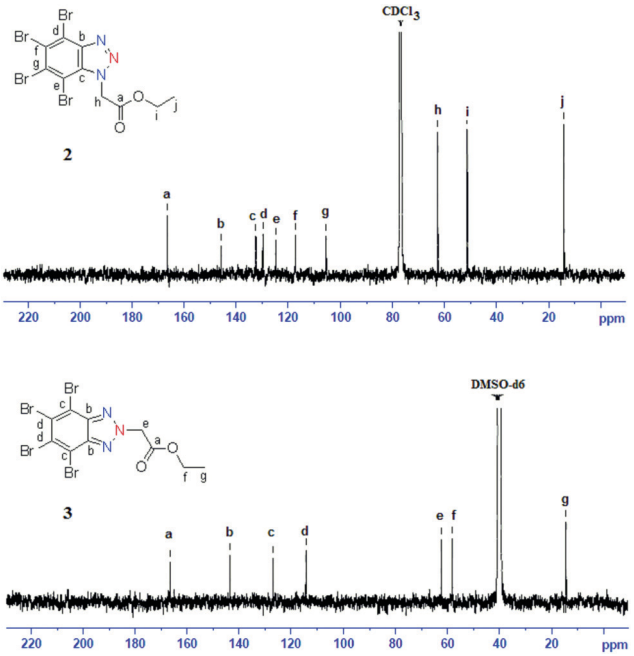

Fig. 2 ^{13}C-NMR spectra demonstrate distinct patterns for purified regioisomers **2** and **3**.

or Ile 174 (7). Moreover, the hydrazide group of **5** and carboxyl group of **7** are super-positioned as the carboxyl group of CX-4945 (Fig. 3b). Both compounds have their hydrophilic groups (hydrazide and carboxyl, respectively) substituted at N^2 of the triazole nucleus. The marked decrease in CK2 enzyme inhibition by compounds **4** and **6** compared to their corresponding isomers (**5** and **7**) may be explained by the loss of direct binding of **4** to Asp175 and water mediated binding of **6** to Trp176 and Glu81 due to changing the position of hydrophilic groups (carboxyl and hydrazide) from N^2 to N^1 of the triazole nucleus. Similarly, esterification of the carboxylic acid group in compound **2** and **3** leads to loss of the direct essential inhibitory hydrogen bonding to Val 116 and water-bridged bonding to Glu81 and Trp176. In the N^2 regioisomers there was no difference in the mode of binding of the hydrazide group in **5** and the carboxyl group in **7**. However, there was a variation between them in the N^1 isomers. As shown in ESI† S1c, the hydrazide group in **4** could not establish a direct bond to Asp175, while the carboxyl group in **6** does not establish an indirect interaction with Glu81 and Trp176 *via* a water molecule. This may explain the converging IC_{50} of **5** and **7** (0.098 μM and 0.13 μM, respectively), and the variable IC_{50} in **4** and **6** (0.39 μM and 0.54 μM, respectively). The docking results are consistent with the concentration dependent CK2α inhibition of the tested compounds and their order of inhibitory activity (**2** < **5** < **7**) as shown in Fig. 3d. Both the CK2α inhibition assay and docking studies illustrated clearly that the nature and position of the substituting groups of the tested compounds are critical factors for the interaction of the tested compounds with the CK2 enzyme.

2.3. *In vitro* anti-proliferative activity

The anti-proliferative assay was performed against human breast and lung adenocarcinoma cell lines (MCF-7 and A549, respectively), using the 3-(4,5-dimethylthiazol-2-yl)-2,5-diphenyltetrazolium bromide (MTT) colorimetric assay as described by T. Mosmann.[29] Cell viability of cancer cell lines was evaluated after 48 h treatment with the tested compounds, Fig. 4. The tested compounds exhibited comparable patterns of anti-proliferative activity in both cell lines at 5 μM concentration where the hydrazides (**4** and **5**) were more effective than their corresponding esters (**2** and **3**). A549 cells were slightly more sensitive to the tested compounds than MCF-7 cells, which lack caspase 3 and have impaired apoptosis. Compound **5** demonstrated a significantly higher anti-proliferative effect than its corresponding regioisomer **4**.

All the compounds were tested on MCF-7 at several concentrations in the range of 2.5–20 μM to determine their IC_{50} values (Fig. 4c, f and ESI† S2). IC_{50} is the concentration of a tested compound, which decreases the percentage of viable cells to half in comparison to negative control cells treated with only media and positive control cells treated with doxorubicin as a reference anticancer drug. Compounds **2**, **4**, **6** and **7** demonstrated moderate anti-proliferative activity with IC_{50} for the MCF-7 cell line in the range of 32–37.5 μM, which is markedly better than that of the parent **1**. Compound **3**, which has the ester functional group at N^2 of the triazole ring was more potent with IC_{50} = 23 μM. Compound **5**, which has the hydrazide functional group at N^2 of the triazole ring exhibited the highest potency in MCF-7 and A549 cell lines (IC_{50} = 9.1, and 6.3 μM, respectively, Fig. 4c) and was equipotent to CX-4945, the most successful CK2 inhibitor in clinical trials. It exhibited a concentration-dependent anti-proliferative activity in both cancer cell lines at a concentration range (0–20 μM) as shown in Fig. 4f.

2.4. Quantitative real-time PCR evaluation of apoptotic gene expression levels

Bax and Bcl-2 are two genes playing opposing roles in the regulation of cellular apoptosis. Their expression leads to two different proteins: Bax (pro-apoptotic) and bcl-2 (anti-apoptotic). In this study, the levels of mRNA expression of Bax and Bcl-2 genes in MCF-7 cells, treated with the tested compounds at 10 μM, were determined using the quantitative real-time PCR (qRT-PCR) technique. Interestingly, all the treated cells (Fig. 4d and e) exhibited increase of the Bax mRNA expression levels (upregulation) and non-significant change of Bcl-2 m-RNA expression levels. Both the hydrazide derivatives (**4–5**) showed four to five times higher levels of Bax m-RNA than the corresponding ester (**3**) or acid (**7**). The most potent compound (**4**) demonstrated a concentration-dependent up-regulation of Bax m-RNA (Fig. 4g) with non-significant change in Bcl-2 m-RNA expression levels (Fig. 4h) at the tested concentration range (0–20 μM).

A comparison of the results from the CK2 enzyme inhibition (Fig. 3a) and anti-proliferative activity (Fig. 4c) gave different order of activity for the tested compounds. For instance, both the hydrazide (**5**) and the acid (**7**) achieved similar levels of CK2 enzyme inhibition, which are three times more potent than that of the corresponding ester **3**. The hydrazide **5** was significantly more cytotoxic and apoptotic than both **3** and **7** (Fig. 4d and e). The difference between CK2 enzyme inhibition and cytotoxic

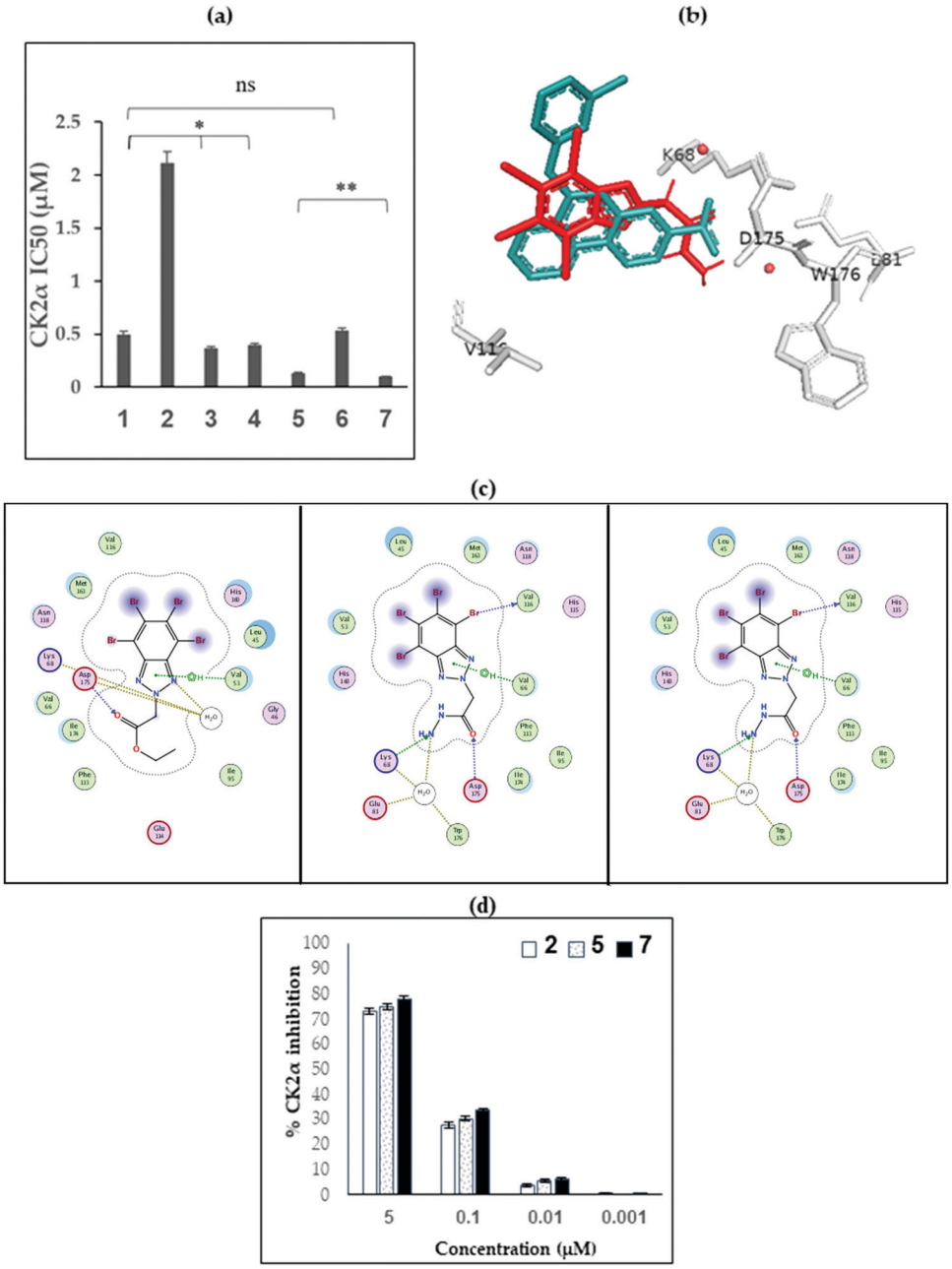

Fig. 3 (a) CK2 IC_{50} values of the tested compounds (**1–7**) represented as mean ± SD of three independent experiments statistically analyzed using a *t*-test, **; $p < 0.0$, *; $p < 0.05$, ns; $p > 0.05$), (b) superposition of CX-4945 and compound (**5**) at the ATP binding site of human CK2 enzyme PDB code 3PE1, (c) 2D representation of (**2**), (**5**) and (**7**) docked at the ATP binding site of CK2α, and (d) dose dependent CK2α inhibition of the tested compounds (**2**, **5** and **7**) at concentration range 0.0001–5 μM represented as mean ± SD of three independent experiments.

activities is not fully explained. In order to find a possible explanation for these differences, we decided to estimate the lipophilicity of the tested compounds both theoretically and experimentally as lipophilicity may affect cell penetration properties and hence explain the difference between enzyme and cell-based activities.

2.5 Lipophilicity study

Lipophilicity is a physicochemical property that influences pharmacokinetics, pharmacodynamics and toxicity of drugs as a result of its impact on their passive diffusion through biological membranes. According to IUPAC, lipophilicity is the affinity of a compound for a lipophilic environment. It is generally assessed by the distribution behavior of the drug in biphasic systems such as liquid–liquid systems (*e.g.* 1-octanol/water) or solid–liquid systems (*e.g.* RP-HPLC or RP-TLC).[30] A common parameter used for expression of the lipophilicity of a drug molecule is the partition coefficient, *P*, which represents partitioning of a drug between an aqueous and a non-aqueous phase. The 1-octanol/water solvent system has been recognized

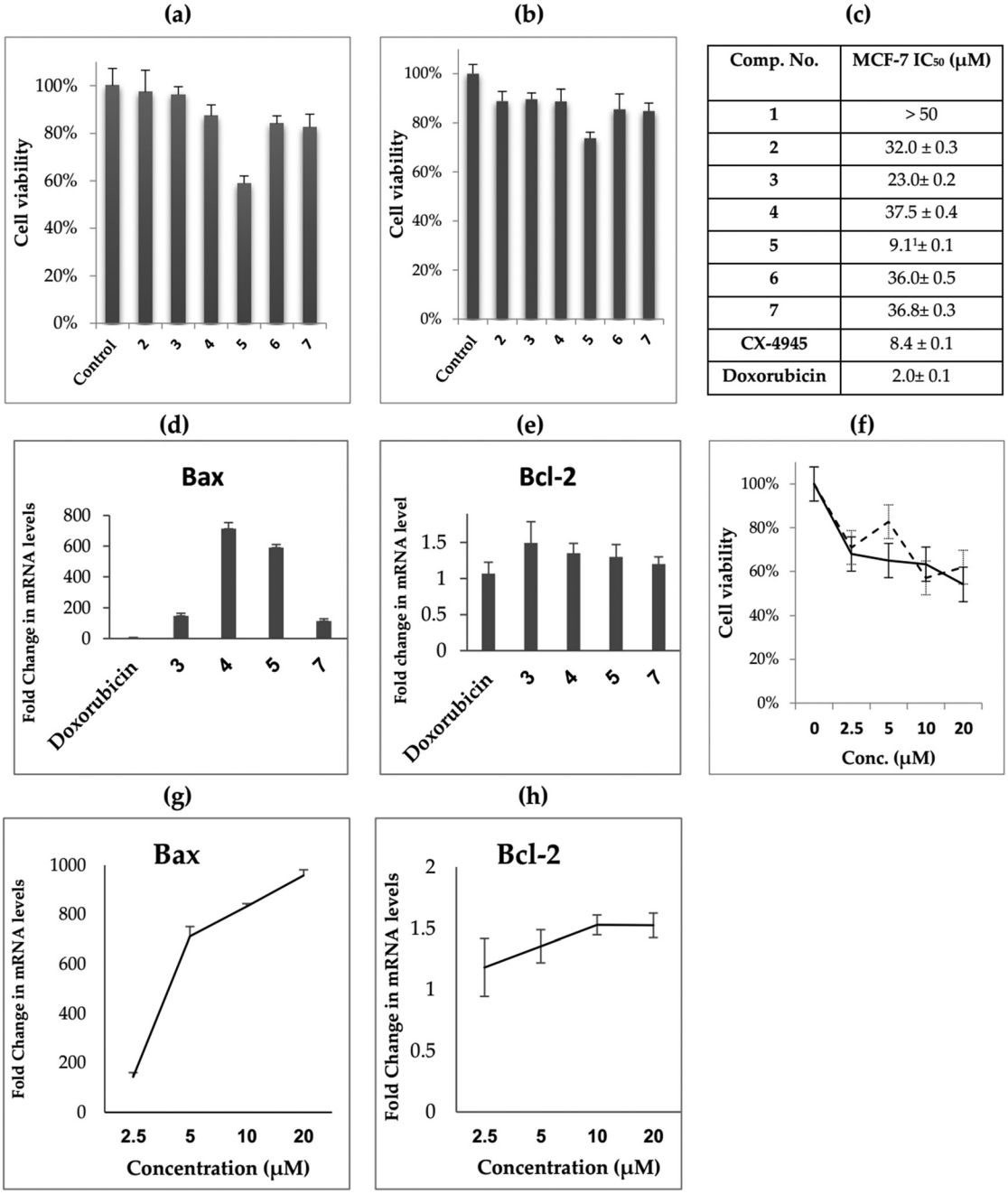

Comp. No.	MCF-7 IC_{50} (μM)
1	> 50
2	32.0 ± 0.3
3	23.0± 0.2
4	37.5 ± 0.4
5	9.1[1]± 0.1
6	36.0± 0.5
7	36.8± 0.3
CX-4945	8.4 ± 0.1
Doxorubicin	2.0± 0.1

Fig. 4 Antiproliferative activities of the tested compounds: (a) cell viability of human lung cancer cell line (A549) treated with the tested compounds at 5 μM for 48 h; (b) cell viability of human breast cancer cell line (MCF-7) treated with the tested compounds at 5 μM for 48 h; (c) IC_{50} (MCF-7) of the tested compounds, the [1]IC_{50} (A549) of **5** is 6.31 μM; (d) fold change in expression levels of BAX mRNA following treatment of MCF-7 cells with the tested compounds at 10 μM for 48 h; (e) fold change in expression levels of BCL2 mRNA following treatment of MCF-7 cells with the tested compounds at 10 μM for 48 h; (f) effect of compound **5** concentration on cell viability of cancer cell lines represented by a solid line (A549) and dashed line (MCF-7); (g) effect of compound **4** concentration on BAX mRNA expression; (h) effect of compound **4** concentration on BCL2 mRNA expression.

as the reference system using the shake-flask technique for the determination of the partition coefficient, $P_{O/W}$, of a drug. Lipophilicity is usually expressed as $\log P_{O/W}$, which is defined as the logarithm of the ratio of concentration of a neutral, non-ionized substance, in 1-octanol to that in water.[31]

Due to practical difficulties of the shake-flask method, reversed-phase (RP) chromatography is frequently used for the estimation of lipophilicity of drugs, mainly RP-HPLC and RP-TLC, relying on their retention factors *via* simulating the 1-octanol–water system. RP-TLC offers many advantages over other methods as it is a cost-effective, rapid and high throughput technique, consumes a small volume of solvents and requires simple equipment and hence it is widely used for the experimental estimation of lipophilicity.[32]

Table 1 Calculated log*P* values using the different software programs

	Calcd log $P_{O/W}$			
Comp. no.	MOE	Molsoft	ChemDraw	ALOGPS 2.1
1	4.67	3.91	4.26	3.94
2	4.16	4.05	4.07	4.28
3	4.31	4.44	5.04	4.38
4	2.41	1.92	2.71	3.20
5	2.56	2.31	3.04	3.55
6	3.55	3.22	3.84	3.41
7	3.70	3.62	4.15	3.76

Computation methods using the different computer programs can be used to generate calculated log*P* values for the studied compounds, based on atom contributions, fragment contributions, atom/fragment contributions or atom-type electrotopological-state indices and neural network modeling, for instance, MOE, Molsoft, ChemDraw and ALOGPS.

2.5.1. Theoretical lipophilicity calculation of N^1 and N^2-substituted TBBt derivatives. The lipophilicity of the tested compounds was theoretically calculated using four different software programs (Molsoft, MOE, ChemDraw and ALOGPS 2.1). The calculated log $P_{O/W}$ values of the tested compounds (**1–7**, Table 1) were in the range of 1.92–5.04. The orders of lipophilicity of the tested compounds were different amongst the different software programs. The highest lipophilic compound is the ester derivative (**3**) as calculated by the Molsoft, ChemDraw and ALOGPS 2.1 software programs. The MOE software predicts the parent compound (**1**) to be the most lipophilic in the series. The highest hydrophilic compound as calculated by all the software is the hydrazide derivative (**4**) with calculated log $P_{O/W}$ in the range of 1.92–3.20, which is about one digit less than the calculated values of the acid derivatives (**6** and **7**).

In conclusion, the lipophilicity prediction software programs give contradicting results despite the structural similarity among the tested compounds and are not reliable to comprehend the differences in the antiproliferative activities of the tested compounds. Previous studies on polyhalogenated benzotriazoles and benzimidazoles relied on the calculated lipophilicity values, which may have complicated interpretation of their anticancer activities.[33,34] However to our knowledge there were no attempts to experimentally measure the lipophilicity of any polybrominated benzimidazole or benzotriazole derivatives. We thought the experimental estimation of the lipophilicity of the TBBt derivatives would give unprecedented information and may provide clues about the lipophilicity-antiproliferative activity relationship.

2.5.2. Experimental lipophilicity estimation of N^1 and N^2-substituted TBBt derivatives using RP-TLC. Lipophilicity parameters were experimentally measured using the RP-TLC method as described elsewhere.[31] Three mobile phases were used consisting of different proportions of water and organic modifiers (acetonitrile, acetone and methanol). Briefly, the R_F and R_M values were obtained for each organic modifier/water system ratio (ESI† S3–S5) and a linear regression analysis was achieved to obtain three lipophilicity chromatographic descriptors (R_{M0}, b, and C_0 Table 2).

R_{M0} is known as ''the relative lipophilicity'' as it describes the solute partition between pure water and nonpolar stationary phase. On the other hand, b (slope of the regression line) describes the specific hydrophobic surface area of the compound. In a series of structurally related compounds, b is linearly correlated with R_{M0} resulting in a linear relationship that is the basic feature of the chromatographic determination of lipophilicity. C_0 represents the concentration of an organic modifier in the mobile phase in which the solute is equally distributed between the two phases, in other words, $R_M = 0$, and $R_F = 0.5$. Moreover, C_0 represents the hydrophobicity per unit of the specific hydrophobic surface area and it is considered more reliable in the QSAR analysis as it embraces both the specific hydrophobic surface area of the solute and the chromatographically-measured lipophilicity index (R_{M0}). High values of correlation coefficients were obtained ($r > 0.9831$, ESI† S3–S5) in all the mobile phases, which proves the high significance of the obtained descriptors for estimation of the lipophilicity. The type of organic modifier (methanol, acetonitrile and acetone, ESI† S3–S5) has small influence on relative lipophilicity (expressed as R_{M0}) or lipophilic parameter (C_0). A significant correlation exists between R_{M0} and slope (b) with $r \approx -0.9406$, -0.9958 and -0.8379 in acetonitrile/water, acetone/water and methanol/water, respectively, which suggests a similar chromatographic retention mechanism for this congeneric series of studied derivatives. Moreover, a good correlation was obtained between R_{M0} and the lipophilic parameter C_0 with $r \approx 0.9250$, 0.9820 and 0.8043 in acetonitrile/water, acetone/water and methanol/water, respectively.

Within the same solvent system, the differences in R_{M0} values between the tested compounds are attributed to the variation in their substituents, which affects considerably their lipophilicity. Higher R_{M0} values were found for the relatively lipophilic derivatives containing an ester group (**3** and **2**, Table 2) followed by the hydrazide derivative group (**5**), which was more lipophilic than TBBt itself. N^2 derivatives were slightly more lipophilic than their corresponding N^1 derivatives. This finding

Table 2 RP-TLC measured lipophilicity parameters R_{M0}, b and C_0

	R_{M0}			b			C_0		
Comp. no.	ACN	Acetone	MeOH	ACN	Acetone	MeOH	ACN	Acetone	MeOH
1	2.02	3.16	3.59	−0.0268	−0.0428	−0.0416	75.36	73.77	86.34
2	3.42	4.15	4.01	−0.0404	−0.0512	−0.0429	84.52	81.13	93.64
3	3.64	4.51	4.69	−0.0417	−0.0543	−0.0488	87.27	83.06	96.13
4	1.39	3.07	2.26	−0.0240	−0.0412	−0.0286	57.78	74.53	79.05
5	2.56	3.69	3.88	−0.0326	−0.0470	−0.0438	78.49	78.50	88.55
6	1.45	1.51	2.62	−0.0304	−0.0271	−0.0397	47.79	55.66	65.83
7	1.28	2.11	3.38	−0.0258	−0.0351	−0.0465	49.85	60.06	72.69

is critical in understanding the differences between N^1 and N^2 regioisomers regarding their antiproliferative activity. The lowest values of R_{M0} were obtained for the more hydrophilic derivatives containing hydrazide and carboxylic acid groups (**4**, **7** and **6**, Table 2). Compound **3** (containing ester group) is the most lipophilic compound. It possesses the highest value of R_{M0}, b and C_0 among all the organic modifier/water systems. According to the C_0 values, compound **6** (containing carboxylic acid group) is the most hydrophilic compound followed by its structural isomer (**7**).

The experimental results of lipophilicity were completely different in comparison with the calculated log$P$ values. In contrast to the calculated log$P_{O/W}$, the most lipophilic compounds as measured by the RP-TLC method are the derivatives containing ester groups (**3** and **2**), followed by the hydrazide derivative (**5**), while the most hydrophilic compounds in the series are the derivatives containing carboxylic groups (**6** and **7**) followed by the hydrazide derivative (**4**).

A comparison of the results from the CK2 enzyme inhibition (Fig. 3a), anti-proliferative activity (Fig. 4c) and experimentally estimated lipophilicity (Table 2) reveals that the hydrazide (**5**) and its acid (**7**) are nearly equipotent as CK2 inhibitors but quite different in terms of the lipophilicity and antiproliferative activity. The hydrazide (**5**) is three times more potent as an antiproliferative compound than the acid (**7**), which may be attributed to its increased lipophilicity as it would have better chance to penetrate cell membranes. There is also a significant difference between the two hydrazide regioisomers (**4** and **5**) in terms of lipophilicity, antiproliferative activity and enzyme inhibitory activity. While the ester **3** is more lipophilic than both **5** and **7**, it exhibited reduced cytotoxic response as a result of its reduced enzyme inhibitory activity.

3. Materials and methods

3.1. General

All commercially available solvents and reagents were used without further purification. Melting points were measured on an electrothermal melting point apparatus [Model 9100, UK], and were reported as uncorrected. Pre-coated TLC silica gel plates (Kieselgel 0.25 mm, 60G F254, Merck, Germany) were used for reaction monitoring and TLC silica gel G 60 RP-18 F_{254} aluminum sheets (Merck, Germany) were used for lipophilicity estimation. TLC spots were detected using an ultraviolet lamp at 254 nm wavelength (Spectroline, model CM-10, USA). Infrared spectra (KBr discs) were recorded on a Thermo Scientific Nicolet IS10 FT-IR spectrometer (thermo Fischer scientific, USA) at the Faculty of Science, Assiut University, Assiut, Egypt. ^{1}H-NMR and ^{13}C-NMR spectra were obtained using an AVANCE-III High Performance FT-NMR spectrometer (400 MHz Brucker) at the Faculty of Science, Sohag University, Sohag, Egypt. Mass spectra were obtained using a Direct Probe Controller Inlet Part TO Single Quadrupole Mass Analyzer (Thermo Scientific GCMS Model ISQ LT) using the Thermo X-Calibur software at the Regional Center for Mycology and Biotechnology (RCMB), Faculty of Science, Al-Azhar University, Nasr city, Cairo, Egypt. Elemental microanalyses were performed using an elemental analyzer Model Flash 2000 Thermo Fisher at the Regional Center for Mycology and Biotechnology (RCMB), Faculty of Science, Al-Azhar University, Nasr city, Cairo, Egypt.

3.2. Synthesis

3.2.1. 4,5,6,7-Tetrabromo-1*H*-benzotriazole (1). Synthesis was performed by brominating 1*H*-benzotriazole according to the published method.[28]

3.2.2. Synthesis of N^1 and N^2-acetate esters (2 and 3). Ethyl chloroacetate (2.82 g, 23.0 mmol, and 5 equiv.) was added to a mixture of **1** (2.00 g, 4.6 mmol, and 1.0 equiv.) and K_2CO_3 (1.27 g, 9.20 mmol, and 2 equiv.) and a few crystals of tetrabutylammonium bromide as a phase transfer catalyst in acetone (10 mL). The mixture was stirred at 60 °C for 6 h. The reaction was monitored by TLC and when completed, the solvent was evaporated to dryness. The residue was purified by column chromatography using silica gel and hexane:ethyl acetate (15 : 1 to 7 : 1) as eluent. The two regioisomers (**2** and **3**) were separated in 80% total yield.

*Ethyl(4,5,6,7-tetrabromo-1H-benzo[d]triazol-1-yl)-acetate (**2**).* Yield: 1.15 g (48%), white crystals, m.p. 140 °C. IR (KBr, cm^{-1}): 1734.6 (CO), 2925.2 (C_2H_5). ^{1}H NMR (DMSO-d_6, 400 MHz) δ ppm: 5.89 (s, 2H, CH_2), 4.23 (q, 2H, J = 8.0 Hz, CH_2), 1.24 (t, 3H, J = 4.0 Hz, CH_3). ^{13}C NMR (DMSO-d_6, 100 MHz) δ ppm: 14.07 (CH_3), 51.31 (ester CH_2), 62.67 (N-CH_2), 105.64 (C5), 117.08 (C6), 124.73 (C4), 129.68 (C7), 132.33 (C8), 145.63 (C9), 166.35 (C═O). Anal. calcd/found for $C_{10}H_7Br_4N_3O_2$ (520.723): C, 23.06/23.42; H, 1.35/1.59; N, 8.07/8.24.

*Ethyl(4,5,6,7-tetrabromo-2H-benzo[d]triazol-2-yl)-acetate (**3**).* Yield: 0.766 g (32%), white crystals, m.p. 182–183 °C. IR (KBr, cm^{-1}): 1743.2 (CO), 2967.9 (C_2H_5). ^{1}H NMR (DMSO-d_6, 400 MHz) δ ppm: 5.94 (s, 2H, CH_2), 4.24 (q, 2H, J = 8.0 Hz, CH_2), 1.24 (t, 3H, J = 4.0 Hz, CH_3). ^{13}C NMR (DMSO-d_6, 100 MHz) δ ppm: 14.34 (CH_3), 58.20 (CH_2), 62.50 (N-CH_2), 117.20 (C5 & C6), 126.82 (C4 & C7), 143.37 (C8 & C9), 166.50 (C═O). Anal. calcd/found. for $C_{10}H_7Br_4N_3O_2$ (520.723): C, 23.06/23.27; H, 1.35/1.57; N, 8.07/7.92.

3.2.3. Hydrazinolysis of 2 and 3. A mixture of **2** or **3** (0.120 g, 2.3 mmol, and 1.0 equiv.) and hydrazine hydrate (99%, 0.6 g, 18.5 mmol, and 8.0 equiv.) in ethanol (10 mL) was stirred and refluxed for 6 h. The mixture was left to cool for crystallization and filtered to give pure hydrazide products (**4** or **5**, respectively).

*2-(4,5,6,7-Tetrabromo-1H-benzo[d]triazol-1-yl)acetohydrazide (**4**).* Yield: 0.074 g (63.5%). White crystals, m.p. > 300 °C. IR (KBr, cm^{-1}): 3316.3, 2925.1, 1663.3, 1626.6, 1545.1, 1430.2. ^{1}H NMR (DMSO-d_6, 400 MHz) δ ppm: 4.46 (br s, NH_2), 5.51 (s, CH_2), 9.47 (s, NH). 502.59 (21.03%), 504.32 (14.54%). EI-MS [m/z (%)]: 502.59 (M^+, 21.03%), 504.32 (M^+ + 2,14.54%). Anal. calcd/found for $C_8H_5Br_4N_5O$ (506.774): C, 18.96/19.24; H, 0.99/1.23; N, 13.82/14.09.

*2-(4,5,6,7-Tetrabromo-2H-benzo[d]triazol-2-yl)acetohydrazide (**5**).* Yield: 0.084 g (70.5%). White crystals, m.p. > 300 °C. IR (KBr, cm^{-1}): 3304.2, 3053.5, 2924.0, 1661.4, 1623.6, 1545.9. ^{1}H NMR (DMSO-d_6, 400 MHz) δ ppm: 4.45 (br s, NH_2),

5.51 (s, CH_2), 9.59 (s, NH). ^{13}C NMR (DMSO-d_6, 100 MHz) δ ppm: 58.48 (CH_2), 114.11 (C5 & C6), 126.38 (C4 & C7), 143.27 (C8 & C9), 163.94 (C═O). Anal. calcd/found for $C_8H_5Br_4N_5O$ (506.774): C, 18.96/19.23; H, 0.99/1.07; N, 13.82/14.09.

3.2.4. Base catalyzed hydrolysis of 2 and 3. A suspension of **2** or **3** (0.075 g, mmol) in a solution of 5% NaOH (5 mL) and 2 mL of ethanol was stirred and refluxed for 1 h. The mixture became a clear solution. The solution was brought to pH 2–3 with conc. HCl. The white precipitate was filtered and washed with water to give a pure product (**6** or **7** respectively).

*2-(4,5,6,7-Tetrabromo-1H-benzo[d]triazol-1-yl)acetic acid (**6**).* Yield 0.024 g (33.8%), white crystals m.p. 216 °C. IR (KBr, cm^{-1}): 3200–2500, 3007.4, 296.4, 1736.0, 1630.3. ^{1}H NMR (DMSO-d_6, 400 MHz) δ ppm: 5.77(s, 2H, CH_2). ^{13}C NMR (DMSO-d_6, 100 MHz) δ ppm: 52.1 (CH_2), 97.44, 115.95. Anal. calcd/found for $C_8H_3Br_4N_3O_2$ (492.774): C, 19.50/19.78; H, 0.61/0.87; N, 8.53/8.78.

2-(4,5,6,7-Tetrabromo-2H-benzo[d]triazol-2-yl)acetic acid (7). Yield = 0.025 g (35.2%), white crystals m.p. 263. IR (KBr, cm^{-1}): 3200–2500, 2991.8, 2946.2, 1732.2, 1553.1. ^{1}H NMR (DMSO-d_6, 400 MHz) δ ppm: 5.8 (s, 2H, CH_2). ^{13}C NMR (DMSO-d_6, 100 MHz) δ ppm: 58.47 (CH_2), 114.16 (C5 & C6), 126.60 (C4 & C7), 143.26 (C8 & C9), 167.86 (C═O). Anal. calcd/found for $C_8H_3Br_4N_3O_2$ (492.774): C, 19.50/19.78; H, 0.61/0.87; N, 8.53/8.78.

3.3. CK2α inhibition assay

The CK2α activity was measured by the P81 filter isotopic assay as described elsewhere.[35] Briefly, a reaction solution was prepared using 20 μM substrate peptide (RRRDDDSDDD) and 10 μM ATP dissolved in 40 mM HEPES buffer (50 μL, and pH 7.5) with 130 mM KCl, 10 mM $MgCl_2$, and 50 μM DTT. The enzyme (hCK2α, Sigma-Aldrich) was added to the reaction mixture and was kept for 15 min at 30 °C. 10 μL of the phosphorylation reaction mixture was spotted onto the P81 filter paper followed by washing three times with 0.5% phosphoric acid once with ethanol before scintillation counting. IC50 values for the tested compounds were determined by measuring the CK2α activity at concentrations ranging from 0.001 to 5.0 μM of each compound. All the tested compounds were dissolved in 0.5% DMSO.

3.4. Molecular modelling

All molecular modeling studies were carried out on an Intel(R) Xeon(R) CPU E5-1650 3.20 GHz processor, 16 GB memory with Windows 10 Professional operating system. Molecular Operating Environment (MOE 2014.0901, Chemical Computing Group, Canada) was used as the computational software. Pymol 2.3.2 was used as the viewer. The crystal structure of human protein kinase CK2 catalytic subunit co-crystallized with CX-4945 inhibitor was downloaded from PDB (code: 3pe1). The studied compounds were built using the builder interface of the MOE software and subjected to conformational search. Conformers were subjected to energy minimization until a RMSD gradient of 0.01 kcal mol^{-1} and RMS distance of 0.1 Å with the MMFF94X force-field and the partial charges were automatically calculated. The obtained database was then saved as a MDB file to be used in the docking calculations. Docking of the energy minimized conformations was done using the MOE-dock wizard. London d*G* was used as the scoring function (*S*).

3.5. MTT-based cytotoxicity assay

Cell viability was assessed using the MTT assay as described elsewhere.[29] Briefly, cells were seeded into 96-well tissue culture plates in DMEM containing 10% FBS to a final volume of 200 μL per well. After 24 h of seeding, the cells were treated with the tested compounds, doxorubicin (positive control), or 0.5% DMSO (negative control). After 48 h incubation, the medium was removed and replaced with 200 μL DMEM containing 0.5 mg mL^{-1} MTT. After 2 h incubation, the supernatant was removed, and the precipitated formazan was dissolved in 200 μL DMSO and absorbance measured at 570 nm using a Varioskan flash 4.00.53 microplate reader. All the experiments were performed in six replicates and were calculated by subtracting the blank readings. Tested compounds were screened to find the most active compound(s) capable of significantly influencing cell viability of both cell lines at a low micromolar concentration (5 μM). IC_{50} was calculated as the concentration of the tested compounds required to achieve 50% inhibition of cell viability.

3.6 Evaluating the effect of the tested compounds on the Bax and Bcl2 genes Using Quantitative Real-Time PCR (qRT-PCR)

3.6.1. RNA extraction and reverse transcription. Total RNA was extracted, from MCF-7 cells after overnight treatment with the tested compounds, using the Direct-zol™ RNA MiniPrep (Zymoresearch, Catalog No. R2053, CA, USA). The purity and concentration of RNA were determined using a biotech NanoDrop instrument, and complementary DNA (cDNA) was synthesized using a Thermo Scientific Revert Aid Reverse kit (Thermo, Waltham, MA, US).

3.6.2. Quantitative real-time PCR (qRT-PCR). QRT-PCR was performed using a 7500 Fast Real Time PCR (Applied Biosystems, CA, USA) system using a QuantiTect SYBR Green PCR Kit (Qiagen, Germany) under the following conditions: hot start step at 95 °C for 7 s, initial denaturation for 20 s at 95 °C, and annealing and extension for 60 s at 59 °C for 40 cycles.

The fold change in expression of the Bax and Bcl2 genes was calculated according to the $2^{-\Delta\Delta CT}$ method using β-actin as the internal control gene to normalize the relative level of gene expression. The sequences of the primers used in this study are listed in Table 3.

3.7. Lipophilicity estimation of the tested compounds using the RP-TLC chromatographic method

Chromatographic analysis was carried out on TLC silica gel G 60 RP–18 F_{254} aluminum sheets (20 × 20 cm, and 0.20 mm layer thickness) that were obtained from Merck, Darmstadt, Germany. The mobile phases were prepared by mixing different proportions of double-distilled water and organic modifier. Methanol (SD Fine-Chem Limited, India), acetonitrile (Fisher Scientific U.K. Limited, United Kingdom) and acetone (Merck, Germany) were used as organic modifiers for the preparation of the different

Table 3 Primer sequences of the genes used for qRT-PCR experiments in this study

Genes	Forward primer	Reverse primer
Bax	5′-CCCGAGAGGTCTTTTTCCGAG-3′	5′-CCAGCCCATGATGGTTCTGAT-3′
Bcl2	5′-ATCGCTCTGTGGATGACTGAGTAC-3′	5′-ATCGCTCTGTGGATGACTGAGTAC-3′
β-Actin	5′-TGTTGTCCCTGTATGCCTCT-3′	5′-TAATGTCACGCACGATTTCC-3′

mobile phase systems. Standard solution (0.1 mg mL^{-1}) of each of the studied compounds was prepared in methanol (MeOH). The content of the organic modifier, methanol, acetonitrile or acetone, was varied between 50 and 95% (v/v) with an increment of 5%. The upper and lower content of the organic modifier depends on the linearity between R_M and the organic modifier concentration. The concentration ranges for the tested organic modifiers were used, where the upper value of the range indicates that the analyte elutes near the solvent front and the lower value implies that the analyte is very near to the starting line. Then, the chromatographic chambers were saturated with the mobile phase for 0.5 h. TLC was performed on RP TLC plates (20 × 5 cm pieces). The standard solutions (5 μL) were spotted in triplicate on the plates 5 mm apart, 10 mm from the bottom edges and 5 mm from the side edges. The plates were air-dried and then developed in the chromatographic chambers. Linear ascending plate development was performed until a migration distance of 35 mm from the origin was reached. After development, the plates were removed and air-dried. Then the spots were localized under UV light at λ = 254 nm. Finally, the R_F values were calculated.

R_m values were derived using R_f of solutes in mobile solvent systems including water and an organic modifier such as acetone or methanol followed by construction of a relationship between R_m and C (percentage of organic modifier). A linear regression analysis was carried out using Excel 2016 (Microsoft Office) to obtain the lipophilicity of the chromatographic descriptors (R_{M0}, b, and C_0) as calculated from the following equations.

$$R_M = \log\left(\frac{1}{R_f} - 1\right), \quad R_M = R_{M0} + bC, \quad C_0 = -\frac{R_{M0}}{b}$$

R_{M0} is "the relative lipophilicity" and is obtained by extrapolation of the R_M value to 0% v/v of the organic modifier in the mobile phase system. b is the slope of the regression line. C_0 represents the hydrophobicity per unit of the specific hydrophobic surface area and is the concentration of an organic modifier in the mobile phase for which the solute is equally distributed between the two phases.

4. Conclusions

The current study reports the synthesis, purification and characterization of N^1 and N^2-substituted regioisomers of the most potent CK2 enzyme inhibitor; TBBt. We have shown that incorporation of hydrophilic substituents at N^2 improved TBBt CK2 enzyme inhibition and antiproliferative activities. We are the first to report the experimental estimation of the lipophilicity for TBBt derivatives and its contradiction with their calculated values. This would shed light on the complex relationship between enzyme inhibition, lipophilicity and antiproliferative activity of TBBt derivatives. Further studies are needed to measure the CK2 inhibitory activity of TBBt regioisomers in the treated cells and to determine their CK2 enzyme specificity and their ability to target other kinases. This may improve our understanding of the structure–activity relationships of the TBBt regioisomers and would impact the design of future CK2 based anticancer agents.

Author contributions

Conceptualization and experimental design, A. M. A.; methodology and experiments, A. E., Y. A. M, M. N. A., N. A. H, N. G. M. and H. F. H; data analysis and interpretation, A. E., Y. A. M, M. N. A., N. A. H., H. F. H., N. G. M; A. M. A; manuscript writing A. E., N. G. M, M. N. A., A. M. A.; all authors have read and approved the final manuscript.

Conflicts of interest

There are no conflicts to declare.

Notes and references

1 M. M. Chua, C. E. Ortega, A. Sheikh, M. Lee, H. Abdul-Rassoul, K. L. Hartshorn and I. Dominguez, *Pharmaceuticals*, 2017, **10**(1), 18.
2 A. Shahraki and A. Ebrahimi, *New J. Chem.*, 2019, **43**, 15983–15998.
3 I. M. Hanif, I. M. Hanif, M. A. Shazib, K. A. Ahmad and S. Pervaiz, *Int. J. Biochem. Cell Biol.*, 2010, **42**, 1602–1605.
4 N. P. Shah, C. Tran, F. Y. Lee, P. Chen, D. Norris and C. L. Sawyers, *Science*, 2004, **305**, 399–401.
5 L. J. Lombardo, F. Y. Lee, P. Chen, D. Norris, J. C. Barrish, K. Behnia, S. Castaneda, L. A. Cornelius, J. Das, A. M. Doweyko, C. Fairchild, J. T. Hunt, I. Inigo, K. Johnston, A. Kamath, D. Kan, H. Klei, P. Marathe, S. Pang, R. Peterson, S. Pitt, G. L. Schieven, R. J. Schmidt, J. Tokarski, M. L. Wen, J. Wityak and R. M. Borzilleri, *J. Med. Chem.*, 2004, **47**, 6658–6661.
6 K. S. Bhullar, N. O. Lagarón, E. M. McGowan, I. Parmar, A. Jha, B. P. Hubbard and H. P. V. Rupasinghe, *Mol. Cancer*, 2018, **17**, 48.
7 D. W. Litchfield, *Biochem. J.*, 2003, **369**, 1–15.
8 M. Saravanabhavan, V. N. Badavath, S. Maji, S. Muhammad and M. Sekar, *New J. Chem.*, 2019, **43**, 17231–17240.
9 R. F. Marschke, M. J. Borad, R. W. McFarland, R. H. Alvarez, J. K. Lim, C. S. Padgett, D. D. V. Hoff, S. E. O'Brien and D. W. Northfelt, *J. Clin. Oncol.*, 2011, **29**, 3087.
10 I. Kufareva, B. Bestgen, P. Brear, R. Prudent, B. Laudet, V. Moucadel, M. Ettaoussi, C. F. Sautel, I. Krimm, M. Engel,

O. Filhol, M. L. Borgne, T. Lomberget, C. Cochet and R. Abagyan, *Sci. Rep.*, 2019, **9**, 15893.
11 G. Cozza, *Pharmaceuticals*, 2017, **10**, 1–23.
12 B. Bestgen, Z. Belaid-Choucair, T. Lomberget, M. Le Borgne, O. Filhol and C. Cochet, *Pharmaceuticals*, 2017, **10**(1), 16.
13 A. Siddiqui-Jain, D. Drygin, N. Streiner, P. Chua, F. Pierre, S. E. O'Brien, J. Bliesath, M. Omori, N. Huser, C. Ho, C. Proffitt, M. K. Schwaebe, D. M. Ryckman, W. G. Rice and K. Anderes, *Cancer Res.*, 2010, **70**, 10288–10298.
14 J. Zhang, P. L. Yang and N. S. Gray, *Nat. Rev. Cancer*, 2009, **9**, 28–39.
15 P. Cohen, *Nat. Rev. Drug Discovery*, 2002, **1**, 309–315.
16 J. Dancey and E. A. Sausville, *Nat. Rev. Drug Discovery*, 2003, **2**, 296–313.
17 A. K. Jain, C. Karthikeyan, K. D. McIntosh, A. K. Tiwari, P. Trivedi and A. DuttKonar, *New J. Chem.*, 2019, **43**, 1202–1215.
18 M. A. Pagano, F. Meggio, M. Ruzzene, M. Andrzejewska, Z. Kazimierczuk and L. A. Pinna, *Biochem. Biophys. Res. Commun.*, 2004, **321**, 1040–1044.
19 P. Zień, M. Bretner, K. Zastąpiło, R. Szyszka and D. Shugar, *Biochem. Biophys. Res. Commun.*, 2003, **306**, 129–133.
20 M. A. Pagano, M. Andrzejewska, M. Ruzzene, S. Sarno, L. Cesaro, J. Bain, M. Elliott, F. Meggio, Z. Kazimierczuk and L. A. Pinna, *J. Med. Chem.*, 2004, **47**, 6239–6247.
21 P. Zien, J. S. Duncan, J. Skierski, M. Bretner, D. W. Litchfield and D. Shugar, *Biochim. Biophys. Acta*, 2005, **1754**, 271–280.
22 H. R. Stefania Sarnoa, F. Meggioa, M. Ruzzenea, S. P. Daviesb, D. S. Arianna Donella-Deanaa and L. A. Pinnaa, *FEBS Lett.*, 2001, **496**(1), 44–48.
23 R. Battistutta, E. D. Moliner, S. Sarno, G. Zanotti and L. A. Pinna, *Protein Sci.*, 2001, **10**, 2200–2206.
24 R. Wąsik, M. Łebska, K. Felczak, J. Poznański and D. Shugar, *J. Phys. Chem. B*, 2010, **114**, 10601–10611.
25 P. Borowiecki, A. M. Wawro, P. Winska, M. Wielechowska and M. Bretner, *Eur. J. Med. Chem.*, 2014, **84**, 364–374.
26 A. D. Ferguson, P. R. Sheth, A. D. Basso, S. Paliwal, K. Gray, T. O. Fischmann and H. V. Le, *FEBS Lett.*, 2011, **585**, 104–110.
27 R. Battistutta, G. Cozza, F. Pierre, E. Papinutto, G. Lolli, S. Sarno, S. E. O'Brien, A. Siddiqui-Jain, M. Haddach, K. Anderes, D. M. Ryckman, F. Meggio and L. A. Pinna, *Biochemistry*, 2011, **50**, 8478–8488.
28 R. Szyszka, N. Grankowski, K. Felczak and D. Shugar, *Biochem. Biophys. Res. Commun.*, 1995, **208**, 418–424.
29 T. Mosmann, *J. Immunol. Methods*, 1983, **65**, 55–63.
30 Ł. Komsta, M. Waksmundzka-Hajnos and J. Sherma, *Thin-Layer Chromatography Drug Analysis*, 2014.
31 S. Šegan, D. Opsenica and D. Milojković-Opsenica, *J. Liq. Chromatogr. Relat. Technol.*, 2019, **42**, 238–248.
32 R. Mannhold, K. Dross, C. Sonntag, V. Pliška, B. Testa and H. van de Waterbeemd, *Lipophilicity in Drug Action and Toxicology*, 1996.
33 E. Łukowska-Chojnacka, P. Wińska, M. Wielechowska, M. Poprzeczko and M. Bretner, *Bioorg. Med. Chem.*, 2016, **24**, 735–741.
34 K. Chojnacki, P. Wińska, K. Skierka, M. Wielechowska and M. Bretner, *Bioorg. Chem.*, 2017, **72**, 1–10.
35 B. B. Olsen, T. Rasmussen, K. Niefind and O. G. Issinger, *Mol. Cell. Biochem.*, 2008, **316**, 37–47.